DEPARTMENT OF PHYSICS

University of Strathclyde Science

PH450 Report 2021-22

Evaluating Spot Finding Methods

Submitted in partial fulfilment for the degree of MPhys

Anton Gashi
Registration No.: 201914462

SUPA Department of Physics, University of Strathclyde, Glasgow G4 0NG, United Kingdom

Dr Sebastian Van De Linde (Primary Supervisor) and Dr Daniel Oi, (Secondary Supervisor)
(Dated: 29th March 2022)

Abstract

Acknowledgements

Contents

List of Figures

List of Tables

I. Introduction

A. Sub-Pixel Localisation

Super-resolution microscopy is the process of taking the diffraction limit of a microscope, 250nm in the x and y direction, and improving it at a minimum by a factor of 2 although more modern methods improve it by up to a factor of 10. In the past this has been achieved by ensemble techniques like SIM (Structured Illumination Microscopy) and STED (Stimulated Emission Depletion) **insert explanation of ensemble techniques**. An improvement on these methods is single-molecule microscopy, in which molecules are individually fluoresced and imaged instead of ensembles which helps distinguish more detail and produce better results than the diffraction limit. There are two ways that this general method have been implemented; photo-activated localization microscopy(PALM) and stochastic optical reconstruction microscopy(STORM), both rely on fluorophores which are fluorescent chemicals that re-emit light after being excited. This helps as the fluorescence emits the light stochastically so only a subset of molecules "light-up" at once, this is important as if they are separated by at least 200nm then they can be located to nanometre precision. Since the molecules are now separated spatially this process needs to just needs to be repeated until all molecules have been "switched-on", this gives a stack of images with blurry spots which can be located and recombined into a final image with spot-precision on the order of $<$ 20nm.[1] The resolution of a super-resolution image usually doesn't refer to the spot-precision of the located molecule, rather it refers to the structural resolution, this can be calculated along with the density of fluorophores as the Nyquist-Shannon sampling theorem states a minimum number of fluorophores are required to resolve the structure (equation 2). [2][3]

1. Pixels and Resolution

In the Modern Dictionary of Electronics by Graf a pixel is described as a, spatial resolution element. The smallest distinguishable and resolvable area in an image. [4] This was mainly in reference to an analog image but the principle applies to a raster image, which is a $N \cdot M$ matrix of values that display colour and intensity. In the specific case of the spot localisation that the Methods section (II) describe the images are $N \cdot N$ and 16-bit black and white.

Resolution is the capability of resolving two points or lines. Since super-resolution by definition changes the resolution of the input images, the resolution of the output image needs to be quantified. Firstly the uncertainty of a spatial measurement is set by the equation;

$$\sigma_{x,y} \sim \frac{\sigma_{PSF}}{\sqrt{N}} \tag{1}$$

Where σ_{PSF} is the standard deviation of the point spread function (PSF) for the microscope, and N is the number of detected photons per florescent event. Since the relationship of equation 1 is approximately the inverse square root, the more detected photons the lower the uncertainty becomes.[5] One of the ways to do this is by using the Nyquist-Shannon sampling theorem, this states that any detail in a measurement that is smaller than twice the size of the average label to label distance can reliably be resolved.[6] The Nyquist resolution limit can be written formally as;

$$\text{Nyquist resolution limit } = \frac{2}{N^{\frac{1}{D}}} \tag{2}$$

Where N is the density of labels, and D is the dimensionality. Labels in this specific case refers to each individual fluorescent event that is detected by the camera, the density of labels is sometimes constrained by the molecules being detected as if the structure that's trying to be detected is too

sparse the uncertainty remains relatively high. For example if the resolution was required to be 20nm in one dimension then fluorophores have to be separated at least 10nm apart at a density of $10^4 \mu m^{-2}$ at a minimum to achieve it. The final resulting uncertainty of the image is therefor the maximum of either equation (1) or (2).

2. Fluorophores

Single molecule super-resolution demands the switching of fluorophores stochastically, this can be done reversibly or irreversibly. Reversible switching fluorophores are photo-activated and emit light until it becomes non-fluorescent again unless reactivated. Irreversible switching fluorophores either start in the off state or the on state, if it starts in an off state it can be photo-activated and turned on then after a period of time it becomes bleached. If it starts switched on then it can be further excited and transition to a red-shifted state.[2]

According to equation 2 the resolution is increased if the number density N is increased, although in order to locate or find a spot in a diffraction limited image the spots need to be spaced apart. Therefor the rate at which populations are on or off can be denoted by k_{on} and k_{off}, also the rate at which the fluorophores switch to the on and off states matter and are denoted as τ_{on} and τ_{off}. The switch rates are directly linked with how many excitations can be detected at once and thus are linked with the ability to accurately find the location of each spot. Ratios between on and off states are denoted as $r = \frac{k_{off}}{k_{on}} = \frac{\tau_{off}}{\tau_{on}}$, the larger the ratio, r, the more accurate results can be up until a point.

B. Motivation

The main motivation behind my project is to improve the compute time that it takes to render images through sub-pixel localisation whilst keeping an acceptable level of accuracy. That is to say this project should be aiming to produce a method of spot-finding that either less complex, less computations per localisation, fewer steps or a mixture of all.

The applications of spot finding reach far beyond localisation microscopy it can be used in other technologies, for example a paper published by Castorena and Creusere [7] has the problem of needing a fast super-resolution technique to get higher spatial resolution from their LIDAR (Light Detection and Ranging) system. This system is constrained by the laser spot size and precision of the scanning mechanical unit as the single laser source with sampling rates in the GHz range which achieves high accuracy for depth and range resolution but poor spatial resolution. A consideration was to decrease the diameter of the laser thus increasing the spatial sampling density, although this was deemed too computationally expensive.

With the almost exponentially increasing launching of small form factor satellites such as the CubeSat, arises the challenge of efficiently utilising the satellites computing resources. This means any segment of code being ran on the satellite needs to run as quickly as possible whilst keeping a certain standard of accuracy, especially for the processes that the satellite depends on to operate like attitude control, power management and calculations for orbital maneuvers. The main method used for orienting(attitude control) CubSat like satellites is by using a Star Tracker, this works by using a camera mounted facing stars that are known to the satellite via a star catalogue and moves based on how aligned or unaligned a reference image is with the actual image seen.[8] The method in which the image is processed so it can be compared to the reference is called spot finding, this entails taking the image and finding each bright spot or star accurately. The motivation for this project is to develop a spot finding method for star tracking and compare it to the state of the art algorithms measuring accuracy, precision and speed.

This technique is also used for super-resolution microscopy, which changes the optical limits of

microscopy from 250nm to about 10nm, this is achieved by temporally or spatially spacing the light coming from the specimen being imaged.

still need to add more technologies that use spot localisation

C. Literature Review (don't call it literature review)

The field of spot finding or star finding is a fairly recent field with papers coming out in the mid 80's from NASA. However the methods haven't changed that much since the main algorithm still used is centroiding since it's a very good compromise between quickness and accuracy being that it can give an answer in the 1-100 microsecond range [9]. Much of the innovation has come from optimising the algorithm or optimising the data going into the algorithm.

II. Methods

A. Centroiding

The most common way of spot finding for star tracking is to use centroiding algorithms, this is when a subsection of pixels are considered to be a star using a rough calculation. The area of interest is then filtered in such a way that reduces noise and aberrations, finally apply the algorithm in this case it's the center of gravity method (3)(or the moment method)[9][10].

$$(x_b, y_b) = \left(\frac{\sum_{ij} I_{ij} x_{ij}}{\sum_{ij} I_{ij}}, \frac{\sum_{ij} I_{ij} y_{ij}}{\sum_{ij} I_{ij}} \right) \tag{3}$$

As can be seen in equation 3 the centroiding method is fairly trivial, the part that determines the computational operations needed is the i and j terms. These terms are the 'window' of pixels that have been chosen by another rough estimator to get a generalised position, the window is a square around the estimated position so the computation scales like n^2, where n is the window size.[10]

B. Fitting methods

1. Point Spread Function

Point Spread Functions(PSF) is the way an object blurs due to the imaging of a point source of light, it's the reason the diffraction limit of a microscope is 250nm (in the x,y direction) and $>$450-700nm (in the z direction).[1] The PSF is also the smallest resolvable detail that can be seen with light as other objects that emit light that are smaller than one another all appear to be the same size. Provided that laboratory equipment is set up correctly, i.e. the lens is corrected for aberrations and constants are known such as aperture and angels between lens and samples, methods like the Richards-Wolf model and Gibson-Lanni model will calculate the centre of a spot near perfectly. The problem with these methods is that they are complicated and slow, and also offer an answer that is unnecessarily accurate. [11][12]

2. Gaussian

Where the exact prediction of section (II B 1) fails Gaussian fitting tries to succeed by presuming that, if all equipment is set up correctly, the centre of a PSF of a point source is always going to be

in the centre. Thus for 2-D spot finding that can't afford the computational time of the previous method uses the more simple equation:

$$I(x,y) = I_0 \cdot \exp\Big(-a \cdot k^2((x-x_0)^2 + (y-y_0)^2)\Big) + b$$

Where k is $\frac{2\pi}{\lambda}$, a is the width of the PSF, I_0 is the peak intensity and b is the average background per pixel. [12]

3. Triangular method

The triangle method being used takes inspiration from the Gaussian method, in which, a Gaussian curve is produced and the area is calculated by integrating the function. After this the position of the spot is estimated by a hyper-parameter optimisation method which minimises the residual area left over from the fitting process. This triangle method looks to reduce the computational load by removing the integration step, this can be done as the area of a triangle is just $\frac{1}{2}\, base \cdot height$. On top of this, the method also sums pixel intensities across axis, firstly it gives a better signal to noise ratio but also it means the triangle only needs to be rendered in 2 dimensions instead of 3, further reducing the computational time.

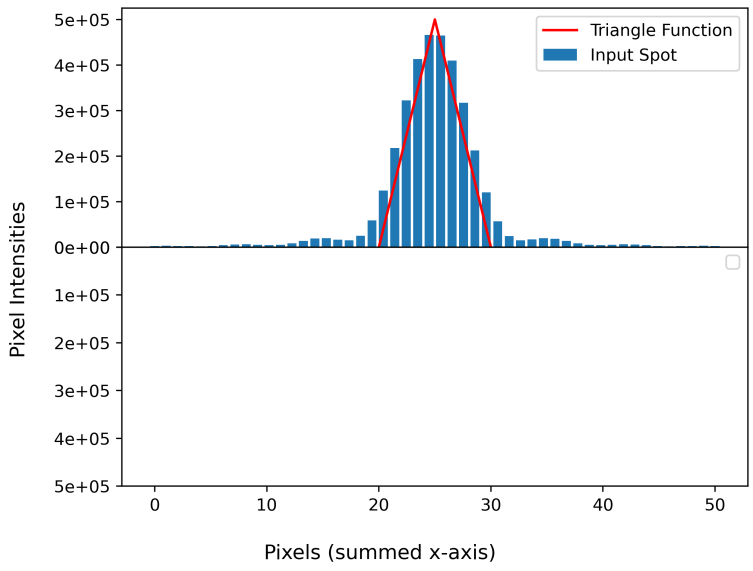

Figure 1. Graph of ideal spot data

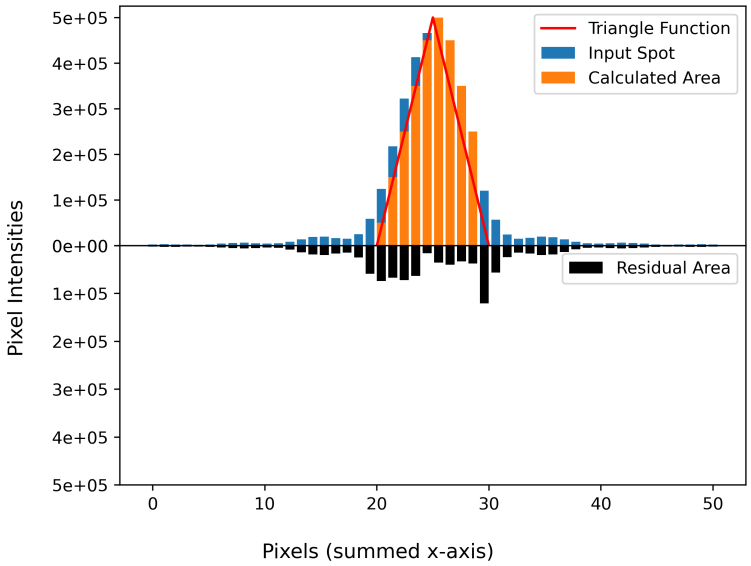

Figure 2. Graph of data from figure 1 with the calculated area and residual

As can be seen in figure 2 the area of the simulated spot are subtracted from the area under the triangle and a residual is left over, this residual parameter is the variable to be minimised for in the optimisation routine.

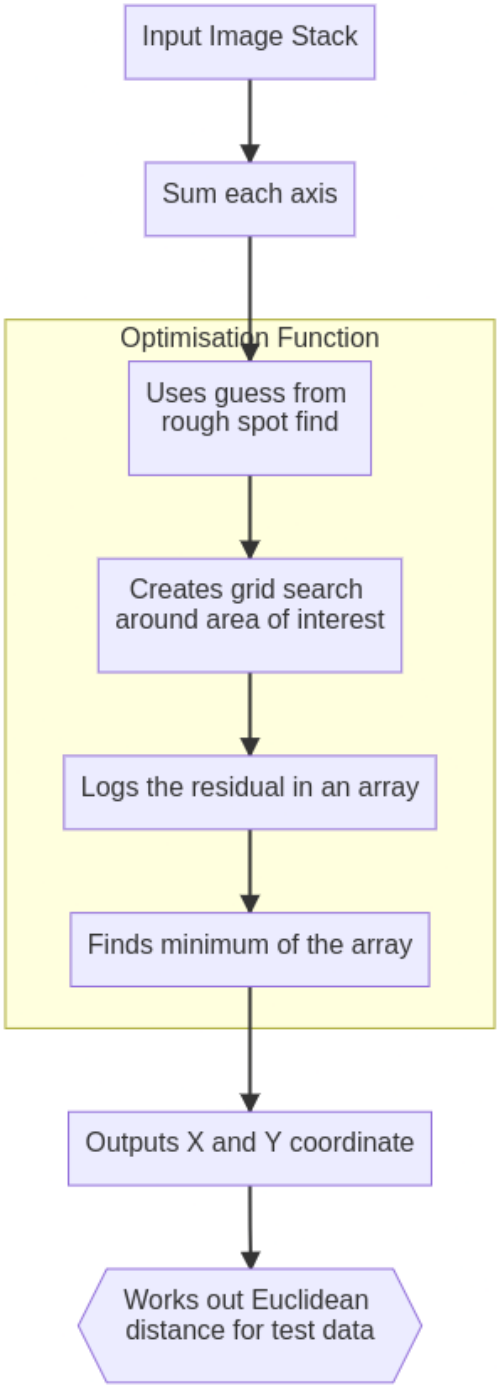

Figure 3. Flowchart describing how the code for the triangular fitting method works

Once the triangle algorithm was implemented it was tested on TIFF stacks of 100 images of perfect spot data. The absolute error (Euclidean distance) was calculated from each axis and plotted as seen in figure 4 A. In image B a histogram was produced so that the spread was more visible.

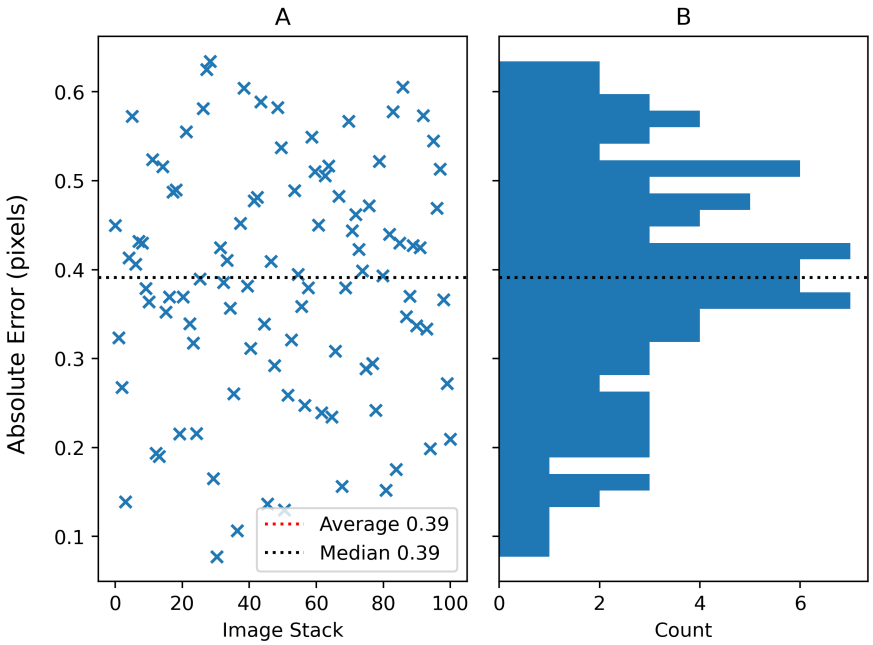

Figure 4. A: Absolute error from the ground-truth for R1.00, B: A histogram of errors from graph A

III. Results and analysis

A. Centroiding

For the centroiding method box sizes of 3, 5, 7 and 11 were used in the production of the histograms pertaining to the absolute error, this was done for the noisy data as well. The rest of the data not presented in the main body of text is available in the appendix section (A).

The results of the centroiding algorithm in figure 5 show a fairly poor level of accuracy, ranging from a $0 \rightarrow 1.5$ pixel error approximately. This lack of accuracy is especially pronounced the larger the radii of spot, the reason for this increasing error is due to the spots being larger in the same sized 50x50 images. The radii of the airy disk that was used to generate the spots is 'physically' larger than the box size that the centroiding is using. This holds true for the radii that are larger than R1.5 as the box size's diameter, as well as the diameter of the airy disk, is 3 pixels. The further increase of inaccuracy seen in figure 5 R4.00, R5.66 and R8.00 is due to the 3x3 box being placed roughly where the centre of the spot already is, then the algorithm is ran which in essence takes the average of the intensities. This 3x3 box is not given a reasonable range of intensities to average over thus the method will be less likely to give the correct answer, this instead gives a range of answers from $0 \rightarrow 1.5$ pixels approximately as if the local maximum finder roughly gives an answer the centroiding algorithm will only give and answer that is 1.5 pixels off of that guess. Since in this perfect data that only has one spot per image, the local maximum finder will predict where the spot is to a single pixel of accuracy thus the maximum error seen should indeed be fractionally larger than 1.5 pixels as observed.

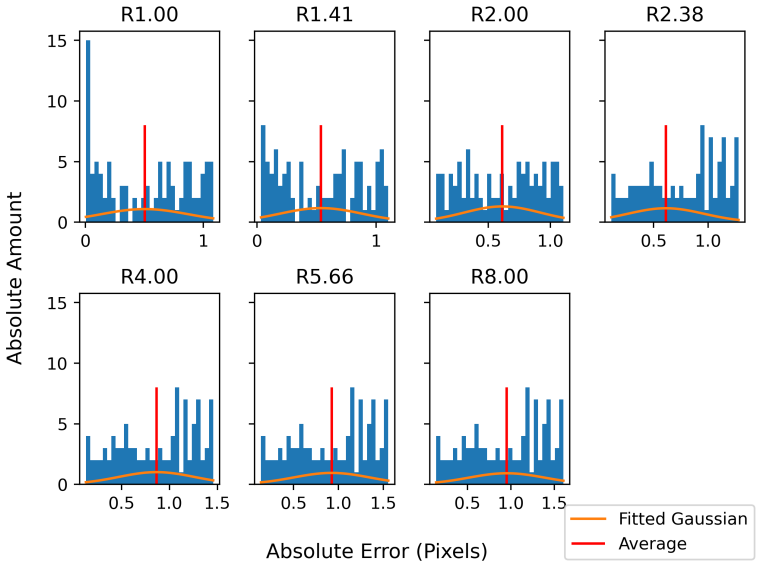

Figure 5. Histograms of the absolute error from each radii with a box size of 3x3 pixels. Completed in 0.19s

In figure 6 noisy spot data was provided to test out the algorithms on, these spot were the same as before but with read noise at 1 electron, average photon number per spot at 2000 and dark current at 0.1 electron per pixel and cg? Also the number of radii were reduced, R1.00 and R1.41 were removed. These noise values were chosen to replicate real world noise levels in order to test all algorithms in isolation from any other variables so that the spot finding methods could be objectively observed.

The noisy data for the 3x3 centroid box size did not have a pronounced impact on average accuracy per radii. This again is due to the size of the box being small relative to the size of the spots, thus mostly not allowing the noise to play a part in the calculation of the centre of the spot. One difference that the noisy data does seem to show is that it gives a more even spread of answers around it's average, this suggests that although the noisy data is not changing the average it is having an effect on the centroiding algorithm. The limiting factor in this case is the box size in which the algorithm is interested in.

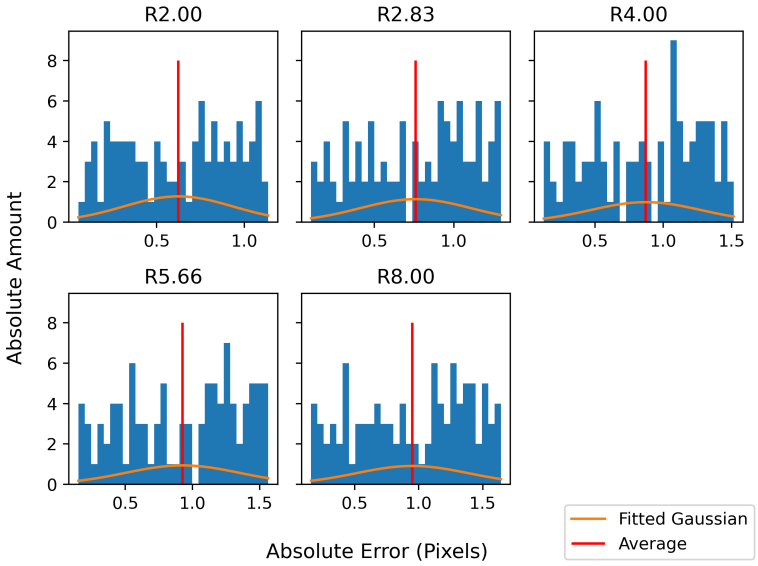

Figure 6. Histograms of the absolute error from each radii with a box size of 3x3 pixels, also with noise.

In figure 7 the box size used was 11x11, this increases the sub-pixel localisation drastically compared to figure 5. The spread of all answers is smaller using 11x11 instead of using 3x3 boxes, the spread also changes with radii sequentially getting larger along with the average. This is due to the larger box size being able to fit more pixels in to average over effectively, this is clearly evident in the R5.66 and R8.00 histogram as there is a significant jump in inaccuracy as the radii is still larger than the radii of the box.

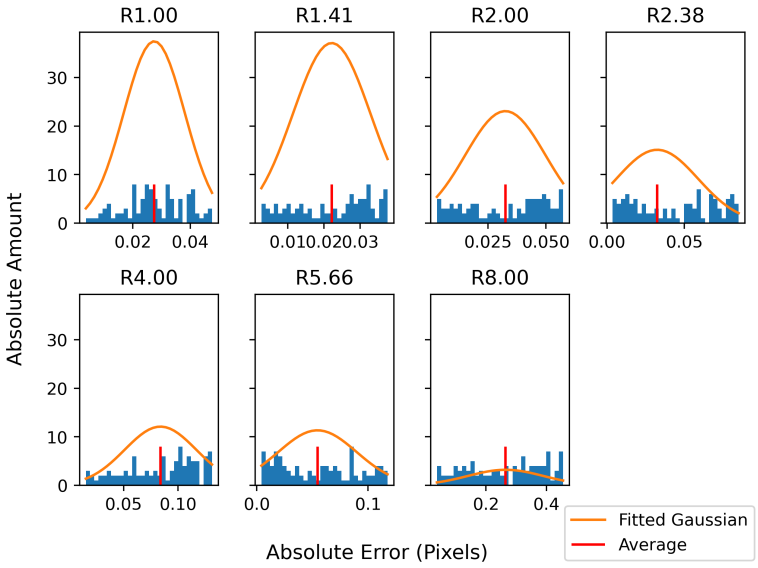

Figure 7. Histograms of the absolute error from each radii with a box size of 11x11 pixels.

In figure 8 when centroiding was used on the noisy data with an 11x11 box size, on average the accuracy decreased as expected and gave a similar average error for each radii apart from R8.00. Again this will be due to the fact that the R8.00 spot will not fit into the box size being calculated but also in relation to the spot, as the size of the spot increases so to does the noise in the images provided.

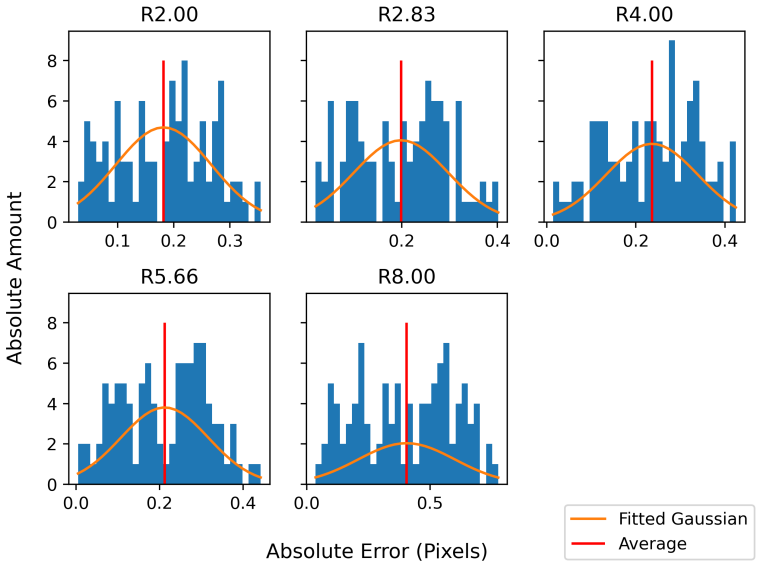

Figure 8. Histograms of the absolute error from each radii with a box size of 11x11 pixels, also with noise.

In figure 9 the box size for making the centroiding calculation was varied from 3 to 49 pixels^2 in odd increments, this was tested to understand the relationship between box size and accuracy. In general the larger the box size the more accuracy gained this was expected especially for the perfect data as there was only one spot per image, although this would be impractical for real data as spot are more than likely to be closer than ≈ 15 pixels. **try and talk about the sin nature of the plot**

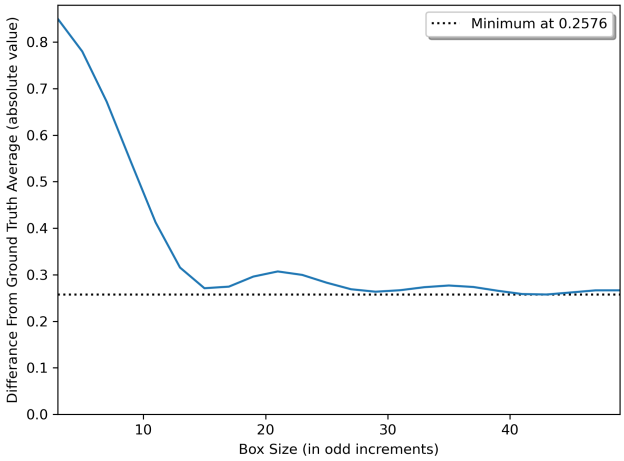

Figure 9. Showing the accuracy of centroiding Vs the box size chosen, for a radii or R8.00.

Figure 10, similar to figure 9, shows the accuracy of the centroid method against the varying box size, but on a set of noisy data. Here it can be seen that for a period of box size increases the accuracy also increases, then it minimises and then decreases indefinitely. Presumably this specific box size minimises the error at ≈ 15 pixels due to the radii being R8.00, as each spot seems to be most optimised at double it's radii. This makes sense as if the centre is what the algorithm is looking for then it should look exactly where that spot is ideally, presuming there are other artefacts in the image like noise.

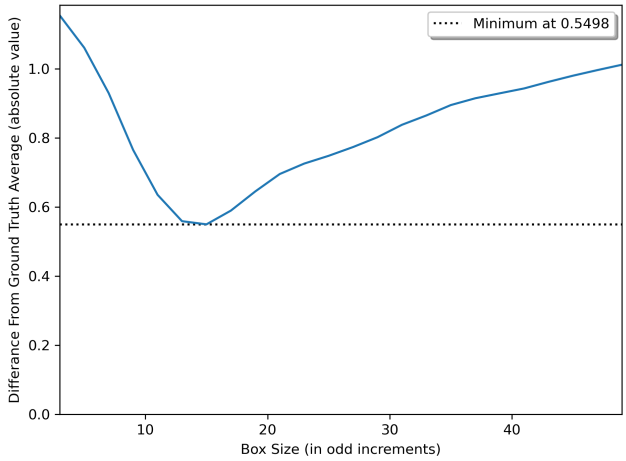

Figure 10. Showing the accuracy of centroiding Vs the box size chosen, for a radii or R8.00 and with noise

B. Triangle Fitting

In figure 17 it can be seen that while using simulated data the mean accuracy of the localisation is 0.4 of a pixel whilst being executed in 0.34s.

Part C of figure 17 has been replicated for all simulated spots given in figure 18 to compare how the change in spot size changes accuracy.

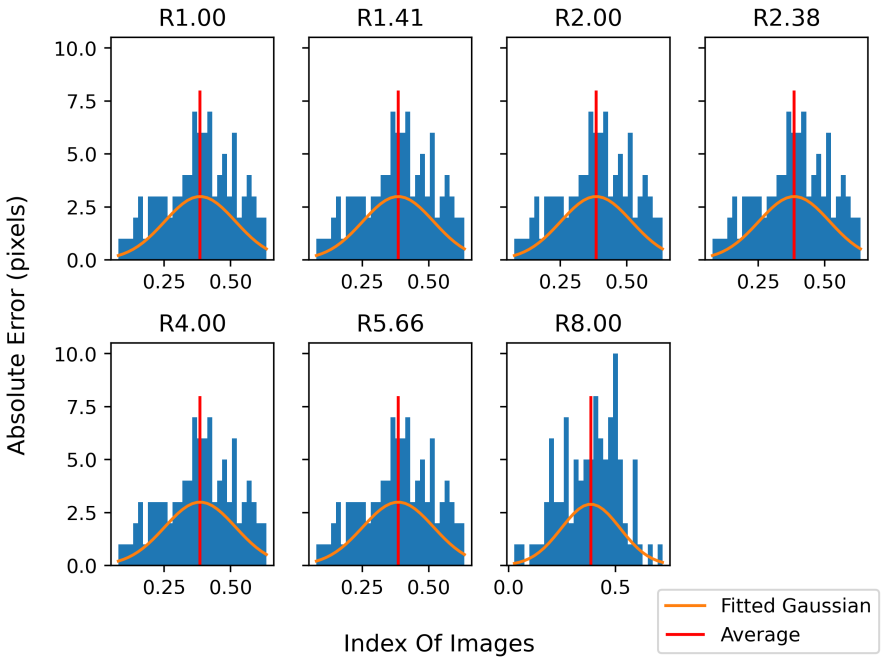

Figure 11. Histograms of the absolute error from each radii

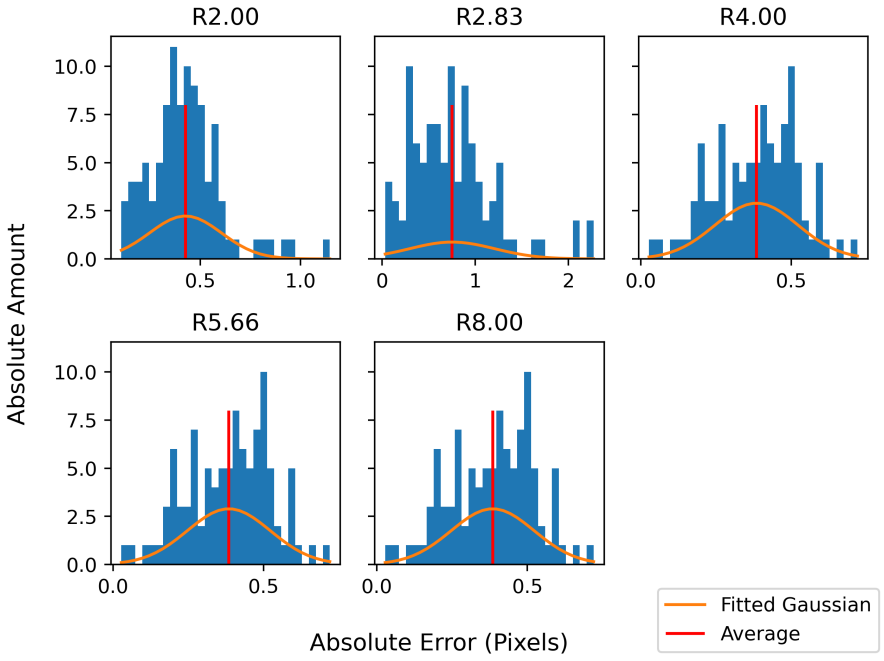

Figure 12. Histograms of the absolute error from each radii, but with noise

As can be seen in figure 12, compared with figure 11, the distribution of results is shifted towards being less accurate. This is expected as noise adds randomness and variability into the system, giving extra information that does not aid in the process of finding the centre of a spot.

IV. Discussion

A. Results in context of my aims

B. Results in comparison with other studies/industry standard

C. Explanations for unexpected results

D. Discuss improvements

V. Conclusion

To conclude

References

[1] Catherine G Galbraith and James A Galbraith. Super-resolution microscopy at a glance. *Journal of cell science*, 124(10):1607–1611, 2011.

[2] Sebastian van de Linde, Steve Wolter, and Markus Sauer. Single-molecule photoswitching and localization1. *Australian Journal of Chemistry*, 64(5):503–511, 2011.

[3] Claude Elwood Shannon. Communication in the presence of noise. *Proceedings of the IRE*, 37(1):10–21, 1949.

[4] R.F. Graf. *Modern Dictionary of Electronics*. Newnes, 1997.

[5] Graham T. Dempsey. Chapter 24 - a user's guide to localization-based super-resolution fluorescence imaging. In Greenfield Sluder and David E. Wolf, editors, *Digital Microscopy*, volume 114 of *Methods in Cell Biology*, pages 561–592. Academic Press, 2013.

[6] Philip Tinnefeld, Christian Eggeling, and Stefan W Hell. *Far-field optical nanoscopy*, volume 14. Springer, 2015.

[7] Juan Castorena and Charles D. Creusere. Sub-spot localization for spatial super-resolved lidar. In *2013 IEEE International Conference on Acoustics, Speech and Signal Processing*, pages 2227–2231, 2013.

[8] Nico Calitz. *The design and implementation of a stellar gyroscope for accurate angular rate estimation on CubeSats*. PhD thesis, Stellenbosch: Stellenbosch University, 2015.

[9] Tjorven Delabie, Joris De Schutter, and Bart Vandenbussche. An accurate and efficient gaussian fit centroiding algorithm for star trackers. *The Journal of the Astronautical Sciences*, 61(1):60–84, 2014.

[10] Ronald C Stone. A comparison of digital centering algorithms. *The Astronomical Journal*, 97:1227–1237, 1989.

[11] Bernard Richards and Emil Wolf. Electromagnetic diffraction in optical systems, ii. structure of the image field in an aplanatic system. *Proceedings of the Royal Society of London. Series A. Mathematical and Physical Sciences*, 253(1274):358–379, 1959.

[12] Alex Small and Shane Stahlheber. Fluorophore localization algorithms for super-resolution microscopy. *Nature methods*, 11(3):267–279, 2014.

A. Appendix

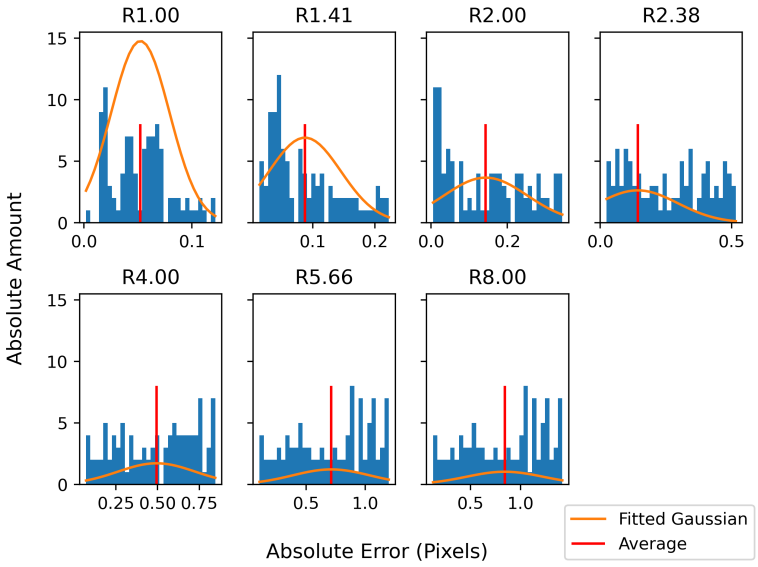

Figure 13.

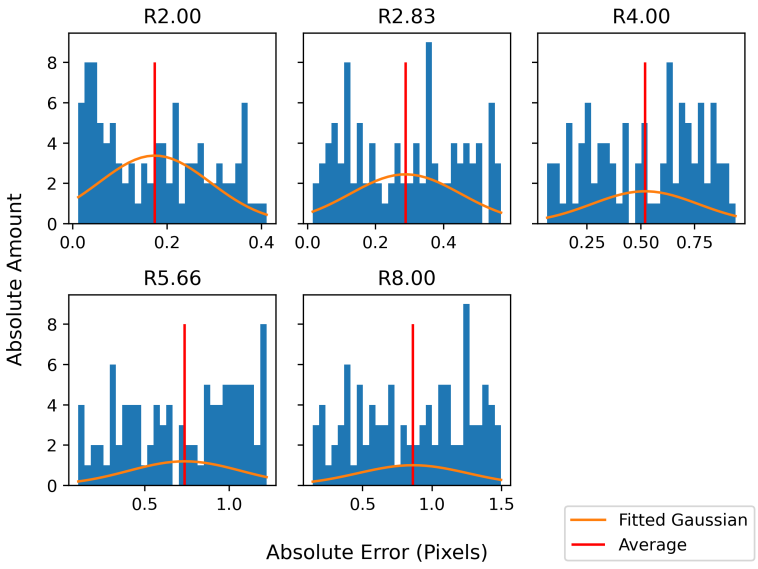

Figure 14.

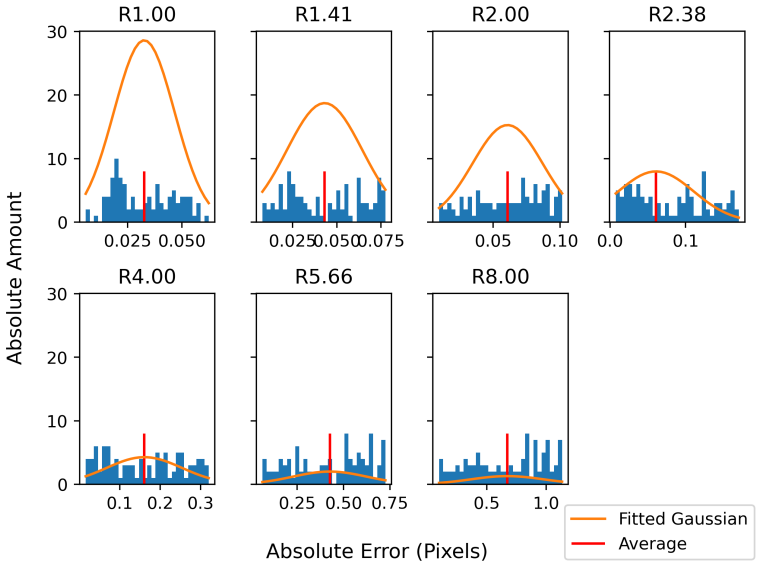

Figure 15.

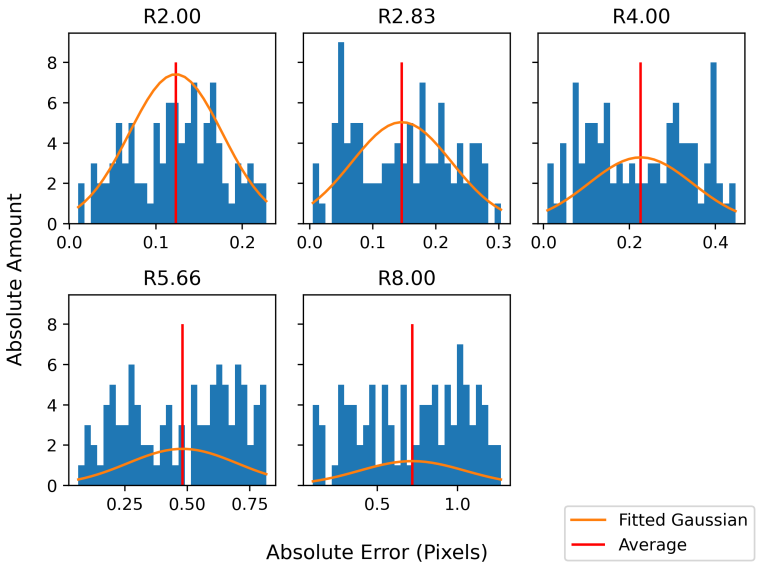

Figure 16.

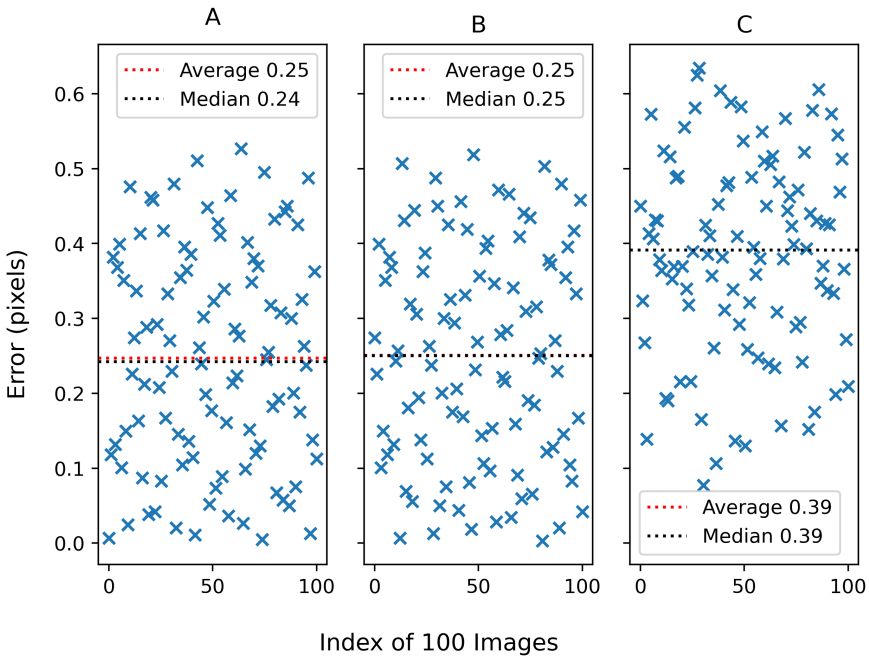

Figure 17. Simulated spots with R1.00, A: Error in the X direction, B: Error in the Y direction, C: Absolute error from the ground-truth

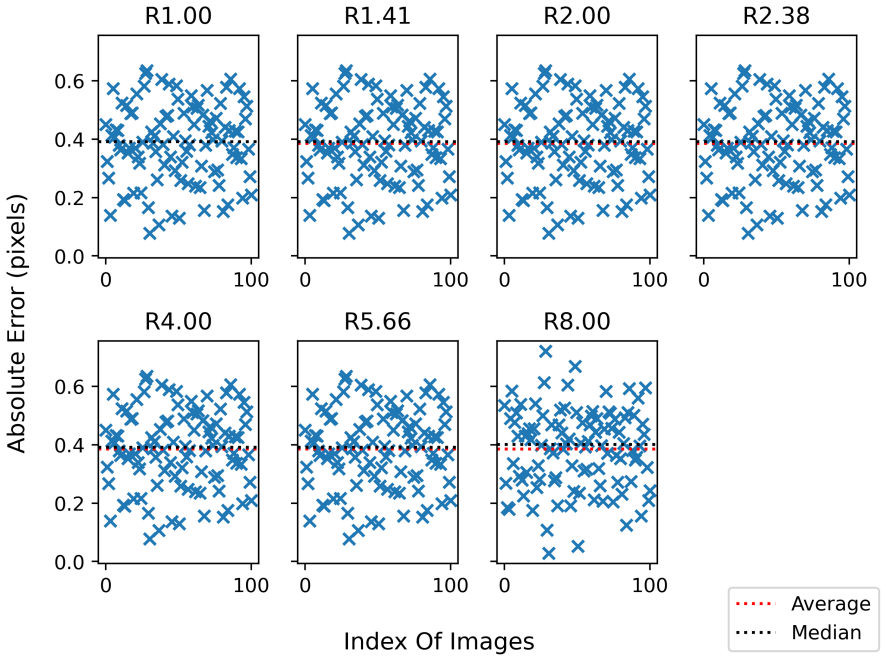

Figure 18. Spot localisation (like graph C in figure 17) of different radii, R, on perfect data (executed in 2.4s)

Radii	Average	Variance
1.00	0.3850	0.0177
1.41	0.3850	0.0177
2.00	0.3850	0.0177
2.83	0.3850	0.0177
4.00	0.3850	0.0177
5.66	0.3850	0.0177
8.00	0.3847	0.0189

Table I. Values of figure 11